J. Indian Chem. Soc.,
Vol. 96, May 2019, pp. 599-606

Palladium(II) complex with 1-(2-pyridylazo)-2-naphthol (PAN): Synthesis, X-ray structure, electrochemistry, DFT computation and DNA binding study

Chandan Kumar Manna, Rahul Naskar and Tapan Kumar Mondal*

Department of Chemistry, Jadavpur University, Kolkata-700 032, India

E-mail: tapank.mondal@jadavpuruniversity.in

Manuscript received online 01 April 2019, revised 16 April 2019, accepted 28 April 2019

Herein, we reports a simple approach for the synthesis of a palladium(II) complex with 1-(2-pyridylazo)-2-naphthol (PAN). The complex is characterized by several spectroscopic techniques. The structure is confirmed by single crystal X-ray diffraction method. The interaction of the complex with CT-DNA isinvestigated by UV-Vis method and binding constant is found to be 3.9×10^4 M^{-1}. Competitive binding titration with ethidium bromide (EB) by fluorescence titration method reveals that the complex efficiently displaces EB from EB-DNA system and the Stern-Volmer dynamic quenching constant, K_{sv} is found to be 1.55×10^4 M^{-1}. Electronic structure and UV-Vis spectrum of the complex are well interpreted by DFT and TDDFT calculations.

Keywords: Palladium(II) complex, X-ray structure, electrochemistry, DNA binding study, DFT calculation.

Introduction

Metal-based antitumor drugs like cisplatin, fulvestrant, goserelin, stilboestro, carboplatin and oxaliplatin are widely used in clinics[1–4], but there are some limitations due to the drug resistance over a period of time and adverse side effects[5–8]. These problems have stimulated a far-reaching search and encouraged chemists to develop alternative strategies based on different metals for more efficient, less toxic, and target-specific noncovalent DNA binding anticancer drugs[9,10]. Therefore, attempts are being made to replace cisplatin with suitable alternatives and hence numerous transition metal complexes were tested for their anticancer activity[11–17]. Among the transition metals, palladium(II) complexes which can efficiently bind and cleave DNA under physiological conditions are considered as potential candidates for antitumor drugs due to their structural and thermodynamic similarities to platinum(II) complexes. A number of palladium(II) complexes are developed and examined their potential antitumor activity[18]. Antiproliferative property in breast cancer and normal cells along with the cytotoxic activity and DNA binding property of several palladium(II) complexes are already been reported in literatures[19,20]. DNA and protein are considered as the main targets for anticancer agents, since they are involved in many important mechanisms in cells. The interaction between protein and drugs provides valuable information about the structural features that determine the therapeutic effectiveness and the pharmacological response of drugs[21,22].

Azo compounds are widely used in optical recording devices, molecular switches and photovoltaic devices because of their excellent thermal and optical properties[23–30]. Azo dyes exhibit remarkable biological activities and because of their antibiotic, antifungal and anti-HIV activities they have immense importance in medicinal chemistry[31–33]. Herein, we have used 1-(2-pyridylazo)-2-naphthol (PAN) as ligand which is commonly used as a photometric reagent for wide variety of metal ions and as a metal ion indicator in the complexometric titration. The palladium(II) complex with PAN is synthesized and characterized by several spectroscopic techniques. The structure is confirmed by single crystal X-ray diffraction method and electronic structure is interpreted by DFT calculation. Binding ability of the synthesized palladium(II) complex with CT-DNA has also been explored by UV-Vis and fluorescence method.

Experimental

Materials and methods:

Na_2PdCl_4, n-Bu_4NPF_6 and 1-(2-pyridylazo)-2-naphthol (PAN) were purchased from Sigma Aldrich. All other chemicals and solvents were reagent grade commercial materials and were used without further purification.

Electronic spectra were measured on a Lambda 750 Perkin-Elmer spectrophotometer in methanol. IR spectra were recorded on a RX-1 Perkin-Elmer spectrometer in the range of 4000–400 cm^{-1} with the samples in the form of KBr pellets. Cyclic voltammetric measurements were carried out using a CHI Electrochemical workstation. A platinum wire working electrode, a platinum wire auxiliary electrode and Ag/AgCl reference electrode were used in a standard three-electrode configuration. n-Bu_4NPF_6 was used as the supporting electrolyte in acetonitrile with scan rate of 50 mV s^{-1} under nitrogen atmosphere.

Synthesis of [Pd(PAN)Cl] (1):

0.147 g (0.5 mmol) of Na_2PdCl_4 and 1-(2-pyridylazo)-2-naphthol (PAN) (0.125 g, 0.5 mmol) was refluxed in methanol for 8 h to yield a green solution. The solvent was then removed under reduced pressure in a rotary evaporator. The crude product was further purified by column chromatography using a silica gel (mesh 60–120). The green band of the complex was eluted by 50% (v/v) ethyl acetate-petroleum ether mixture. On removal of the solvent under reduced pressure the pure complex was obtained as a light green solid which was further dried under vacuum. Yield was 0.144 g (74%).

Anal. Calcd. for $C_{15}H_{10}ClN_3OPd$: C, 46.18; H, 2.58; N, 10.77%. Found: C, 46.02; H, 2.51; N, 10.69%; IR data (KBr, cm^{-1}): 1502 υ(C=N), 1411 υ(N=N); ^1H NMR data ($CDCl_3$, ppm): 8.92 (1H, d, *J* 6.2 Hz), 8.27 (1H, d, *J* 7.2 Hz), 7.24–7.94 (7H, m), 6.82 (1H, d, *J* 7.4 Hz); UV-Vis (in CH_2Cl_2), λ_{max} (ε, M^{-1} cm^{-1}): 665 (9765), 616 (9063), 570 (sh.) 440 (7883), 342 (sh.), 306 (11891), 258 (16872). Electrochemistry (in acetonitrile): $E_{1/2}$ = –0.61 V (ΔE = 80 mV) and E_{pc} = –1.38 V.

Crystal structure determination and refinement:

Single crystals of Pd[PAN]Cl (**1**) was grown by slow diffusion of n-hexane into dichloromethane solution of the complex solution at room temperature and at ambient condition for a week. X-Ray data were collected using an automated Bruker AXS Kappa smart Apex-II diffractometer equipped with an Apex-II CCD area detector using a fine focus sealed tube as the radiation source of graphite monochromated Mo Kα radiation (λ = 0.71073 Å). Details of crystal analyses, data collection and structure refinement are summarized in Table 1. Reflection data were recorded using the ω scan technique. The structure was solved and refined by full-matrix least-squares techniques using the SHELX-97[34]. The absorption corrections were done by multi-scan (SHELXTL program package) and all the data were corrected for Lorentz, polarization effect. Hydrogen atoms were included in the refinement process as per the riding model.

Table 1. Crystallographic data and refinement parameters of [Pd(PAN)Cl] (**1**)

Empirical formula	$C_{15}H_{10}ClN_3OPd$
Formula weight	390.11
Crystal system	Monoclinic
Space group	*P*21/*c*
a (Å)	16.621(5)
b (Å)	7.101(5)
c (Å)	19.538(5)
β (°)	23.705(5)
V ($Å^3$)	2741(2)
Z	8
ρ_{calcd} (g cm^{-3})	1.890
μ (mm^{-1})	1.549
T (K)	293(2)
hkl range	–20 to 20, –8 to 8, –28 to 28
F(000)	1536
θ range (°)	2.75 to 25.50
Reflns. collected	39781
Unique reflns. (R_{int})	5092
Observed data ($I > 2\sigma(I)$)	4698
Data/restraints/parameters	5092/0/379
R1, wR2 ($I > 2\sigma(I)$)	0.0379, 0.1262
GOF	1.153
Largest diff. peak/hole (e $Å^{-3}$)	1.390/ –0.981

Computational details:

All computations were performed using the Gaussian09 (G09) program[35]. Full geometry optimization of Pd[PAN]Cl (**1**) was carried out using the DFT/B3LYP method[36,37]. All elements except palladium were assigned the 6-31G(d) basis set. The LanL2DZ basis set with effective core potential was employed for the palladium atom[38–40]. Vibrational frequency calculation was performed to ensure that the optimized geometry was local minima on the potential energy surface. Vertical electronic excitations based on B3LYP optimized geometry was computed using the time dependent density functional theory (TDDFT) formalism[41–43] in dichloromethane using conductor-like polarizable continuum

model (CPCM)[44–46]. GaussSum[47] was used to calculate the fractional contributions of various groups to each molecular orbital.

DNA binding experiments:

Absorption spectral titration:

All experiments involving CT-DNA were performed in Tris-HCl/NaCl buffer solution, pH 7.5. UV-Vis titrations were performed for the complex by keeping the concentration of the complex constant (5.0×10^{-5} *M*) in 1:10 acetonitrile/buffer solution, while varying the concentration of CT-DNA via steady addition of CT-DNA (1.0×10^{-3} *M*). The absorption spectra were recorded in the range of 350–800 nm. CT-DNA solutions were added stepwise until a saturation state was achieved. After each addition, the solutions were allowed to equilibrate for 5 min before collecting the absorption spectra. The equilibrium binding constant (K_b) of the complex with CT-DNA was determined from the spectral titration data using the following eq. (1)[48].

$$\frac{[DNA]}{(\varepsilon_a - \varepsilon_a)} = \frac{[DNA]}{(\varepsilon_b - \varepsilon_f)} + \frac{1}{K_b\,(\varepsilon_b - \varepsilon_f)} \qquad (1)$$

where [DNA] is the concentration of CT-DNA in base pairs, the apparent absorption coefficients ε_a, ε_f and ε_b correspond to A_{obsd}/[complex], to the absorbance for the free palladium(II) complex, and to the absorbance of the palladium(II) complex in the fully bound form, respectively. K_b is the equilibrium binding constant in M^{-1}.

Competitive study with EB by fluorescence method:

The competitive binding study of Pd(II) complex with EB was carried out by fluorescence method in order to understand the efficiency of displacement of EB from CT-DNA-EB system by the Pd(II) complex. The CT-DNA-EB complex was prepared by adding 10 μM EB and 12 μM CT-DNA in Tris-HCl/NaCl buffer solution, pH 7.5. The fluorescence spectra of EB bound to CT-DNA at 607 nm were obtained at an excited wavelength of 530 nm. The intercalating effect of the Pd(II) complex with the DNA-EB was studied by gradual addition of complex solution into the solution of the DNA-EB.

Results and discussion

Synthesis and formulation:

The palladium(II) complex, [Pd(PAN)Cl] (**1**) was synthesized by the reaction of 1-(2-pyridylazo)-2-naphthol (PAN) and Na_2PdCl_4 in 1:1 mole ratio under refluxing condition in methanol solution (Scheme 1). Color of the reaction mixture was changed from red to deep green. The complex was thoroughly characterized by spectroscopic techniques. IR spectrum of the ligand exhibits characteristic peaks of υ(O-H) and υ(N=N) at 3061 and 1433 cm^{-1} respectively but in the complex υ(N=N) stretching is significantly shifted to lower frequency region and is observed at 1411 cm^{-1} suggesting the coordination of the azo-N atom to Pd(II). ^1H NMR signals in $CDCl_3$ is slightly downfield shifted for the complex compare to free ligand values. The structure of complex was confirmed by single crystal X-ray diffraction study.

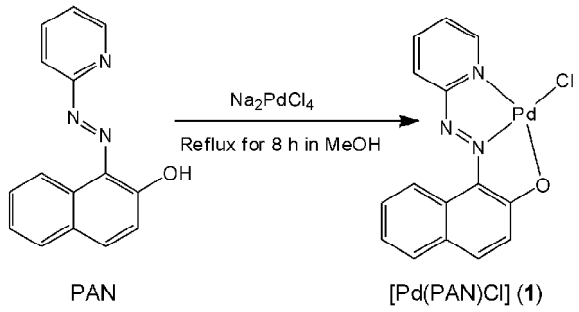

Scheme 1. Synthesis of [Pd(PAN)Cl] (**1**) complex.

Crystal structure

Single crystals suitable for structure determination were obtained by slow diffusion of n-hexane into dichloromethane solution of [Pd(PAN)Cl] (**1**). Crystallographic data collection and refinement parameters are given in Table 1; selected bond lengths and angles are given in Table 2. The perspective view of the molecule along with atomic numbering scheme is shown in Fig. 2. In the complex the geometry about palladium(II) is distorted square planar because of the sig-

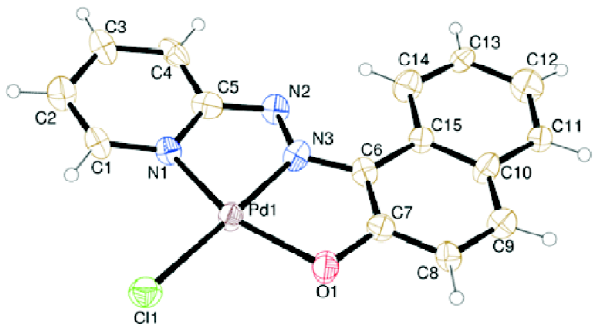

Fig. 1. ORTEP plot 35% ellipsoidal probability of [Pd(PAN)Cl] (**1**).

Table 2. Selected X-ray and calculated bond distances (Å) and angles (°) of **1**

Bonds (Å)	X-Ray	Calcd.
Pd1-Cl1	2.269(4)	2.317
Pd1-O1	2.074(4)	2.061
Pd1-N1	1.958(5)	2.035
Pd1-N3	1.937(3)	1.975
N2-N3	1.293(4)	1.299
O1-C7	1.348(2)	1.288
Angles (°)		
N1-Pd1-N3	79.0(2)	79.406
N1-Pd1-O1	160.5(2)	160.962
N1-Pd1-Cl1	99.3(2)	98.428
N3-Pd1-O1	81.4(2)	81.556
N3-Pd1-Cl1	178.2(2)	177.834
O1-Pd1-Cl1	100.1(2)	100.609

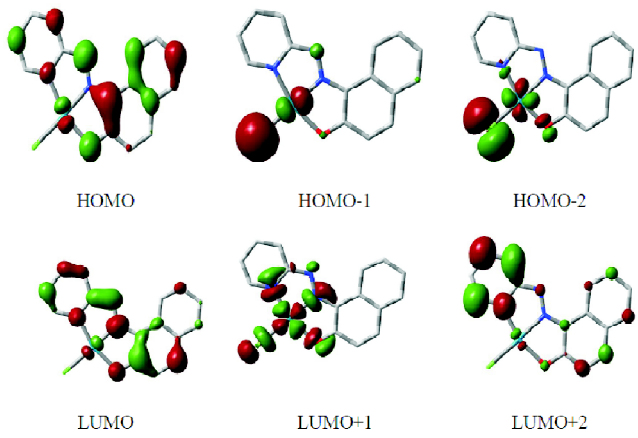

Fig. 2. Contour plots of some selected molecular orbital of **1**.

nificant deviation of chelate bite angles from 90° (N1-Pd1-N3, 79.0(2)° and O1-Pd1-N3, 81.4(2)°). The Pd-N(azo) bond (Pd1-N3, 1.937(3) Å) is slightly shorter than the Pd-N(pyridyl) bond (Pd1-N1, 1.958(5) Å) may be due to strong dπ(Pd) → π* (N=N) back donation in the complex. The Pd1-O1 and Pd1-Cl1 bond distances 2.074(4) and 2.269(4) Å respectively in the complex are found to be as expected[48].

DFT calculation:

The geometry of the complex [Pd(PAN)Cl] (**1**) was fully optimized in singlet ground state by DFT method using B3LYP exchange-correlation functional. The optimized geometric parameters are given in Table 2. The calculated bond parameters are reasonably well reproducing the X-ray crystal structures data. Contour plots of selected molecular orbitals are given in Fig. 3; energy and compositions of selected molecular orbitals are given in Table 3. The higher energy occupied molecular orbital (HOMO) has 92% contribution of PAN. The HOMO-1 and HOMO-2 have 67–75% pπ(Cl) character along with reduced contribution of dπ(Pd) (18–22%). The HOMO-3, HOMO-5 and HOMO-7 are concentrated on (63–93%) PAN while HOMO-4 is contributed by dπ(Pd) or-

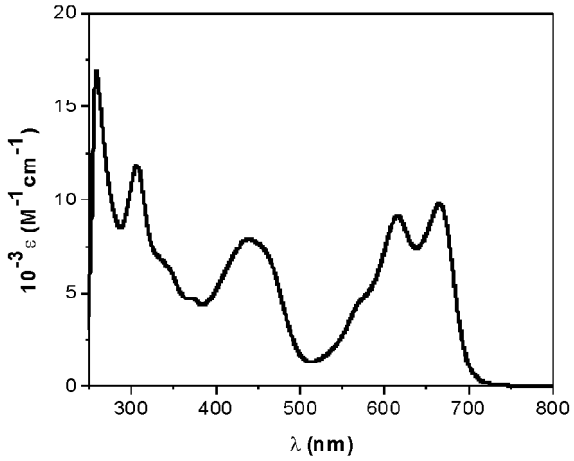

Fig. 3. UV-Vis spectrum of **1** in CH_2Cl_2.

Table 3. Energy and % of composition of some selected molecular orbitals of **1**

MO	Energy (eV)	% Composition		
		Pd	PAN	Cl
LUMO+5	–0.20	02	98	0
LUMO+4	–0.48	01	99	0
LUMO+3	–1.24	0	100	0
LUMO+2	–1.60	02	98	0
LUMO+1	–2.12	53	35	12
LUMO	–3.34	06	93	01
HOMO	–5.93	06	92	02
HOMO-1	–6.41	22	12	67
HOMO-2	–6.46	18	07	75
HOMO-3	–6.74	04	93	03
HOMO-4	–6.95	83	11	06
HOMO-5	–7.48	33	63	04
HOMO-6	–7.57	05	55	40
HOMO-7	–7.70	34	63	03
HOMO-8	–8.01	25	61	14
HOMO-9	–8.37	54	30	16
HOMO-10	–8.77	03	97	00

bitals (83%). The low lying virtual orbital, LUMO has 93% π* (PAN) character while LUMO+1 has 53% dπ(Pd) and 35% π*(PAN) character. The HOMO to LUMO energy gap in the complex is 2.59 eV.

TDDFT calculation and electronic spectra:

The UV-Vis spectrum of the complex in CH_2Cl_2 exhibits low energy closes by peaks at 665 nm (ε, 9765 M^{-1} cm^{-1}), 616 nm (π, 9063 M^{-1} cm^{-1}) and a shoulder peak at 570 nm. A moderately intense broad peak is observed at 440 nm (ε, 7883 M^{-1} cm^{-1}). Sharp ligand centered peaks are observed at 306 nm (ε, 11891 M^{-1} cm^{-1}) and 258 nm (ε, 16872 M^{-1} cm^{-1}) along with a shoulder at 342 nm (Fig. 3).

To get deep insight into the electronic transitions, TDDFT calculation on the optimized geometry of the complex was performed. We found a low energy singlet-singlet vertical excitation at 584 nm corresponds to HOMO→LUMO transition (*f* = 0.2108) having ILCT (intra-ligand charge transfer) character. The experimental band at 440 nm have XLCT (halogen to ligand charge transfer) character ($\lambda_{calcd.}$, 399 nm, *f* = 0.2794). The high energy intense transitions at 306 nm and 258 nm have ILCT character (Table 4).

Electrochemistry:

The electrochemical behavior of the complex was investigated by cyclic voltammetry (CV) in presence of n-Bu_4NPF_6 in acetonitrile solution at scan rate 50 mV s^{-1}. Cyclic voltammogram of the complex exhibits one reversible reduction couple at –0.61 V (Δ*E* = 80 mV) along with an irreversible cathodic reduction peak at –1.38 V (E_{pc}), negative to reference electrode (Ag/AgCl) in the potential range 2.0 to –2.0 V (Fig. 4). The reversible reduction couple at –0.61 V corresponds to $L/L^{\bullet-}$ reduction, and the cathodic peak at –1.38 V corresponds to further reduction of $L^{\bullet-}$ to L^{2-} in the complex.

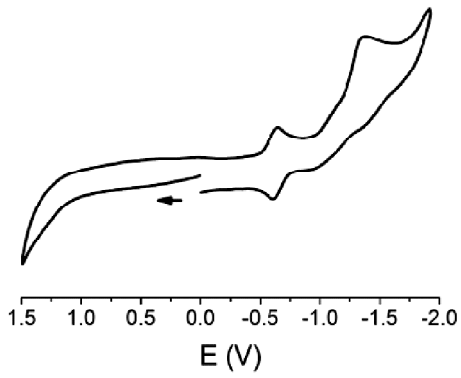

Fig. 4. Cyclic voltammogram of **1** in acetonitrile.

DNA binding studies:

UV-Vis method:

The binding mode and strength of binding of the complex to CT-DNA was studied by using UV-Vis method in Tris buffer solution. UV-Vis method is one of the most useful techniques to study the binding of any drug to DNA. Absorption titration experiments of the Pd(II) complex in buffer solution were performed using a fixed Pd(II) complex concentration (50 μM) to which DNA stock solution were added gradually. The binding of the Pd(II) complex to DNA led to a decrease in the absorption intensity at 436 nm, at 611 and 662 nm (Fig. 5). To quantitatively evaluate the affinity of the Pd(II) complex

Table 4. Vertical electronic transition calculated by TDDFT/CPCM method of **1** in acetonitrile

λ (nm)	*E* (eV)	Osc. strength (*f*)	Key excitations	Character[a]	$\lambda_{expt.}$ (nm) (10^{-3} ε, M^{-1} cm^{-1})
584.0	2.1230	0.2108	(92%) HOMO→LUMO	π(L)→π*(L) ILCT	614
447.3	2.7718	0.2794	(95%) HOMO-1→LUMO	pπ(Cl)/dπ(Pd)→π*(L) XLCT/MLCT	441
331.6	3.7393	0.1163	(73%) HOMO-6→LUMO	π(L)/pπ(Cl)→π*(L) ILCT/XLCT	342 (sh.)
292.1	4.2449	0.2039	(93%) HOMO→LUMO+3	π(L)→π*(L) ILCT	307
259.7	4.7733	0.1334	(43%) HOMO-8→LUMO+2	π(L)→π*(L) ILCT	259

[a]MLCT: Metal to ligand charge transfer; ILCT: Intra-ligand charge transfer and XLCT: Halogen to ligand charge transfer transition.

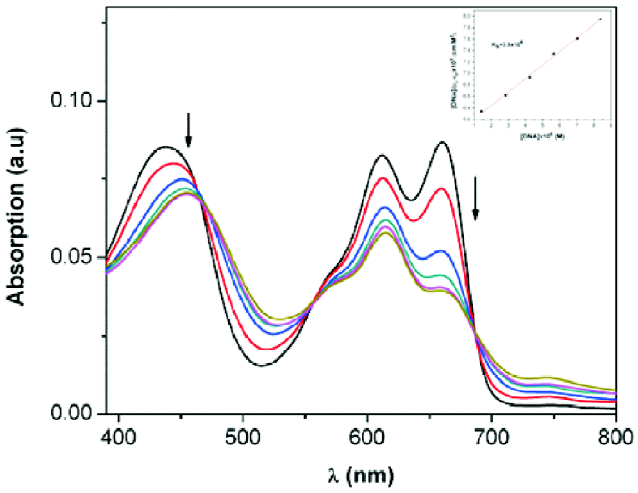

Fig. 5. Change in absorption spectra of **1** in Tris-HCl/NaCl buffer with gradual addition of CT-DNA. Inset: Plot of [DNA]/($\varepsilon_b - \varepsilon_f$) versus [DNA].

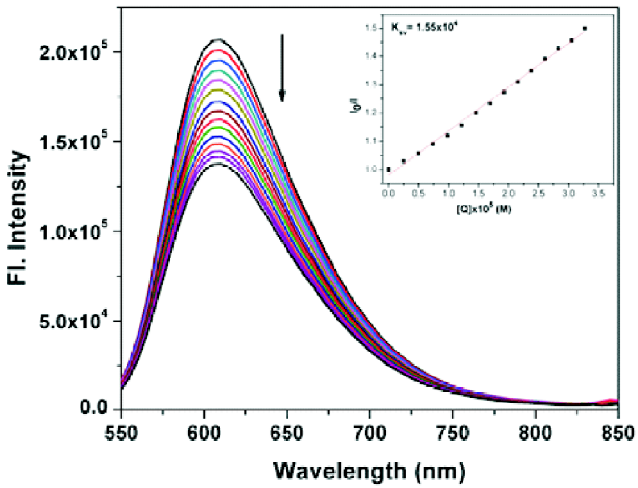

Fig. 6. Emission spectra (λ_{ex} = 540 nm) of EB-CT-DNA in presence of increasing amount of Pd(II) complex **1**. Inset: Plots of emission intensity I_0/I versus Q.

towards DNA we have monitored the change in absorption at 436 nm, the binding constant K_b of the Pd(II) complex to CT-DNA is found to be 3.9×10^4 M^{-1}. This value is comparable to the reported values of binding constants for other Pd(II) complexes towards CT-DNA[49].

Fluorescence method:

Fluorescence method is one of the effective way to study the interaction of metal complexes with CT-DNA. Ethidium bromide (EB) is one of the most sensitive fluorescence probes that can bind to DNA. An enhancement of fluorescence intensity is observed due to the intercalation of EB into CT-DNA. When metal complex intercalates into DNA it leads to a decrease in fluorescence intensity due to the replacement of EB from EB-CT-DNA system. Herein, Pd(II) complex was gradually added to CT-DNA, pre-treated with EB and the fluorescence intensity gradually decreased with the increasing concentration of Pd(II) complex (Fig. 6). This is a clear indication that the complex competes with EB to the binding sites of DNA. The fluorescence quenching curve of the EB-CT-DNA system for the complex is in good agreement with the linear Stern-Volmer equation (eq. (2))[50].

$$I_0/I = 1 + K_{sv}[Q] \quad (2)$$

where, I_0 and I are the fluorescence intensities of the CT-DNA solutions in the absence and in the presence of the complex, respectively. K_{sv} is the Stern-Volmer dynamic quenching constant and [Q] is the total molar concentration of the quencher. K_{sv} is obtained by the slope of the plot and is found to 1.55×10^4 M^{-1}. The moderate value of K_{sv} suggests the Pd(II) complex can displace EB and tightly bound to CT-DNA.

Conclusion

In summary, we have utilized spectroscopic techniques like FT-IR, UV-Vis, ^{1}H NMR and fluorescence to characterize the palladium(II) complex with 1-(2-pyridylazo)-2-naphthol (PAN) and the structure of the complex was confirmed by single crystal X-ray diffraction method. The ability of the complex to bind with CT-DNA is investigated by absorption titration and binding constant found to be 3.9×10^4 M^{-1}. Competitive binding titration with ethidium bromide (EB) by fluorescence method (K_{sv} = 1.55×10^4 M^{-1}) indicated the complex is quite capable to displace EB from EB-DNA. DFT and TDDFT calculations are well interpreted the electronic structure and electronic spectrum of the complex.

Acknowledgement

Financial support received from the Science and Engineering Research Board (SERB), New Delhi, India (EEQ/2018/000226) is gratefully acknowledged. TKM is also grateful to the UGC-CAS II program for financial support.

Supplementary materials

Crystallographic data for the structure of **1** has been deposited with the Cambridge Crystallographic Data Center,

CCDC No. 1576003. Copies of this information may be obtained free of charge from the Director, CCDC, 12 Union Road, Cambridge CB2 1EZ, UK (E-mail: deposit@ccdc.cam.ac.uk or www:htpp://www.ccdc.cam.ac.uk).

References

1. L. Kelland, *Nat. Rev. Cancer*, 2007, **7**, 573.
2. N. P. E. Barry and P. J. Sadler, *Pure Appl. Chem*., 2014, **86**, 1897.
3. C. H. Leung, S. Lin, H.-J. Zhong and D. L. Ma, *Chem. Sci*., 2015, **6**, 871.
4. M. Ashfaq, T. Najam, S. S. A. Shah, M. M. Ahmad, S. Shaheen, R. Tabassum and G. Rivera, *Curr. Med. Chem*., 2014, **21**, 3081.
5. T. Boulikas and M. Vougiouka, *Oncol. Rep*., 2003, **10**, 1663.
6. E. Wong and C. M. Giandomenico, *Chem. Rev*., 1999, **99**, 2451.
7. M. Galanski, V. B. Arion, M. A. Jakupec and B. K. Keppler, *Curr. Pharm. Des*., 2003, **9**, 2078.
8. D. Wang and S. Lippard, *Nat. Rev. Drug Discovery*, 2005, **4**, 307.
9. J. Ruiz, N. Cutillas, C. Vicente, M. D. Villa and G. Lopez, *Inorg. Chem*., 2005, **44**, 7365.
10. E. J. Gao, C. Liu, M. C. Zhu, H. K. Lin, Q. Wu and L. Liu, *Anti-Cancer Agents Med. Chem*., 2009, **9**, 356.
11. S. Halder, S. M. Peng, G. H. Lee, T. Chatterjee, A. Mukherjee, S. Dutta, U. Sanyal and S. Bhattacharya, *New J. Chem.*, 2008, **32**, 105.
12. D. K. Demertzi, M. A. Demertzis, J. R. Miller, C. S. Frampton, J. P. Jasinski and D. X. West, *J. Inorg. Biochem*., 2002, **92**, 137.
13. P. I. Da, S. Maia, A. G. De, A. Fernandes, J. N. Silva, A. D. Andricopulo, S. S. Lemos, E. S. Lang, U. Abram and V. M. Deflon, *J. Inorg. Biochem*., 2010, **104**, 1276.
14. A. I. Matesanz and P. Souza, *J. Inorg. Biochem*., 2007, **101**, 245.
15. A. I. Matesanz, C. Hernández, A. Rodriguez and P. Souza, *J. Inorg. Biochem*., 2011, **105**, 1613.
16. L. Otero, M. Vieites, L. Boiani, A. Denicola, C. Rigol, L. Opazo, C. O. Azar, J. D. Maya, A. Morello, R. L. K. Siegel, O. E. Piro, O. E. Castellano, M. Gonzalez, D. Gambino and H. Cerecetto, *J. Med. Chem*., 2006, **49**, 3322.
17. K. Husain, M. Abid and A. Azam, *Eur. J. Med. Chem*., 2007, **42**, 1300.
18. R. Prabhakaran, S. V. Renukadevi, R. Karvembu, R. Huang, J. Mautz, G. Huttner, R. Subashkumar and K. Natarajan, *Eur. J. Med. Chem*., 2008, **43**, 268.
19. S. Padhye, Z. Afrasiabi, E. Sinn, J. Fok, K. Mehta and N. Rath, *Inorg. Chem*., 2005, **44**, 1154.
20. A. I. Matesanz, J. M. Perez, P. Navarro, J. M. Morcno, E. Colacio and P. Souza, *J. Inorg. Biochem*., 1999, **76**, 29.
21. J. Haribabu, K. Jeyalakshmi, Y. Arun, N. S. P. Bhuvanesh, P. T. Perumal and R. Karvembu, *J. Biol. Inorg. Chem*., 2016, **22**, 461.
22. P. Krishnamoorthy, P. Sathyadevi, R. R. Butorac, A. H. Cowley, N. S. P. Bhuvanesh and N. Dharmaraj, *Dalton Trans*., 2012, **41**, 4423.
23. H. N. Joo, B. hue Le and Y. J. Seo, *Tetrahedron Lett*., 2017, **58**, 679.
24. Y. Chen, C. Li, X. Xu, M. Liu, Y. He, I. Murtaza, D. Zhang, C. Tao, Y. Wang and H. Meng, *ACS Appl. Mater. Interfaces*, 2017, **9**, 7305.
25. V. M. Dembitsky, T. A. Gloriozova and V. V. Poroikov, *Nat. Prod. Bioprospect*, 2017, **7**, 151.
26. S. S. Samanta, A. A. Beharry, O. Sadovski, T. M. McCormick, A. Babalhavaeji, V. Tropepe and G. A. Woolley, *J. Am. Chem. Soc*., 2013, **135**, 9777.
27. K. Maho, T. Shintaro, K. Yutaka, W. Kazuo, N. Toshiyuki and T. Mosahiko, *Jpn. J. Appl. Phys*., 2003, **42**, 1068.
28. P. J. Coelho, L. M. Carvalho, A. M. C. Fonseca and M. M. M. Raposo, *Tetrahedron Lett*., 2006, **47**, 3711.
29. S. Wu, W. Qian, Z. Xia, Y. Zou, S. Wang and S. Shen, *Chem. Phys. Lett*., 2000, **330**, 535.
30. K. G. Yager and C. J. Barrett, *J. Photochem. Photobiol. A*, 2006, **182**, 250.
31. H. Nishiyama and J. I. Ito, *Chem. Commun*., 2010, **46**, 203.
32. T. P. Stanojkovic, D. Kovala Demertzi, A. Primikyri, I. Garcia Santos, A. Castineiras, Z. Juranic and M. A. Demertzis, *J. Inorg. Biochem*., 2010, **104**, 467.
33. H. Sakurai, Y. Kojima, Y. Yoshikawa, K. Kawabe and H. Yasui, *Coord. Chem. Rev*., 2002, **226**, 187.
34. SHELXS97: G. M. Sheldrick, SHELX97, Programs for Crystal Structure Analysis (release 97-2), University of Göttingen, Göttingen, Germany, 1997.
35. Gaussian 09, Revision D.01, M. J. Frisch, G. W. Trucks, H. B. Schlegel, G. E. Scuseria, M. A. Robb, J. R. Cheeseman, G. Scalmani, V. Barone, B. Mennucci, G. A. Petersson, H. Nakatsuji, M. Caricato, X. Li, H. P. Hratchian, A. F. Izmaylov, J. Bloino, G. Zheng, J. L. Sonnenberg, M. Hada, M. Ehara, K. Toyota, R. Fukuda, J. Hasegawa, M. Ishida, T. Nakajima, Y. Honda, O. Kitao, H. Nakai, T. Vreven, J. A. Montgomery (Jr.), J. E. Peralta, F. Ogliaro, M. Bearpark, J. J. Heyd, E. Brothers, K. N. Kudin, V. N. Staroverov, R. Kobayashi, J. Normand, K. Raghavachari, A. Rendell, J. C. Burant, S. S. Iyengar, J. Tomasi, M. Cossi, N. Rega, J. M. Millam, M. Klene, J. E. Knox, J. B. Cross, V. Bakken, C. Adamo, J. Jaramillo, R. Gomperts, R. E. Stratmann, O. Yazyev, A. J. Austin, R. Cammi, C. Pomelli, J. W. Ochterski, R. L. Martin, K. Morokuma, V. G. Zakrzewski, G. A. Voth, P. Salvador, J. J. Dannenberg, S. Dapprich, A. D. Daniels, Ö. Farkas, J. B. Foresman, J. V. Ortiz, J. Cioslowski and D. J. Fox, Gaussian, Inc., Wallingford CT, 2009.
36. A. D. Becke, *J. Chem. Phys*., 1993, **98**, 5648.

37. C. Lee, W. Yang and R. G. Parr, *Phys. Rev. B*, 1988, **37**, 785.
38. P. J. Hay and W. R. Wadt, *J. Chem. Phys*., 1985, **82**, 270.
39. W. R. Wadt and P. J. Hay, *J. Chem. Phys*., 1985, **82**, 284.
40. P. J. Hay and W. R. Wadt, *J. Chem. Phys*., 1985, **82**, 299.
41. R. Bauernschmitt and R. Ahlrichs, *Chem. Phys. Lett*., 1996, **256**, 454.
42. R. E. Stratmann, G. E. Scuseria and M. J. Frisch, *J. Chem. Phys*., 1998, **109**, 8218.
43. M. E. Casida, C. Jamorski, K. C. Casida and D. R. Salahub, *J. Chem. Phys*., 1998, **108**, 4439.
44. V. Barone and M. Cossi, *J. Phys. Chem. A*, 1998, **102**, 1995.
45. M. Cossi and V. Barone, *J. Chem. Phys*., 2001, **115**, 4708.
46. M. Cossi, N. Rega, G. Scalmani and V. Barone, *J. Comput. Chem.*, 2003, **24**, 669.
47. N. M. O'Boyle, A. L. Tenderholt and K. M. Langner, *J. Comput. Chem*., 2008, **29**, 839.
48. S. Biswas, A. K. Pramanik and T. K. Mondal, *J. Mol. Struct*., 2015, **1088**, 28.
49. S. Jana, A. K. Pramanik, C. K. Manna and T. K. Mondal, *Polyhedron*, 2018, **150**, 118.
50. Y. Zhao, J. Zhu, W. He, Z. Yang, Y. Zhu, Y. Li, J. Zhang and Z. Guo, *Chem. Eur. J*., 2006, **12**, 6621.